Original Research Article

# Mixed Compounds of $Cd_{1-x}Mg_xO$ $(0 \leq x \leq 1)$ and their Optoelectronic Properties




## ABSTRACT

The engineering of bandgap in materials is desired to develop new optoelectronic and photonic devices. The structure, electronic and optical properties of MgO (an insulator) mixed with CdO (a semiconductor) in the stoichiometry $Cd_{1-x}Mg_xO$ $(0 \leq x \leq 1)$ are calculated using the ab initio density functional theory. The bond character changes from partial covalent to a more stronger covalent bond as Cd concentration increases in MgO. The dominant covalent bond, coupled with high bulk modulus values predicts that the mixed compounds are hard materials and that Cd and Mg compliments each other to increase the hardness. All the mixed compounds are indirect bandgap materials. The dielectric function and the refractive index shifts to lower energy domain as Cd concentration increases, indicating that the optoelectronic property of the compounds is Cd dependent. The evaluated optoelectronic property predicts the material to be effective for applications in the visible and UV regions of the energy spectrum.


*Keywords*: *Bandgap, covalent bond, dielectric function, refractive index*

## 1. INTRODUCTION

Due to their distinctive physical properties and wide application areas, considerable attention have been devoted to the understanding of the oxides of group II-VI elements. A member of this group is magnesium oxide (MgO). Stoichiometrically, MgO is an insulator with a cubic sodium chloride (NaCl) rock-salt structure. Its band gap ($E_g$) is 7.3 eV. It has high thermal conductivity and melting temperature [1-4]. Another member of this group is cadmium oxide (CdO). It is a semiconductor with a band gap of 0.85 eV at room temperature. Its normal structure is also the cubic sodium chloride (NaCl) rock-salt (see Fig. 1(a)), which can under pressure, undergo a first-order structural phase transition from the NaCl to the cesium-chloride (CsCl) structure [5]. Because CdO is optically transparent and electrically conductive, it is widely used as window for solar cells. It is also used to manufacture thin-film resistors [6,7]. On the other hand, MgO have shown prospect for high-temperature superconductor and ferroelectric material production [8-11]. Thin layers of MgO are used as dielectrics both to improve discharge characteristics and lifetime in plasma screens [2, 12]. It

is a material of choice as antireflection layer in solar cells and as the insulating material for the gates [13] in Insulated Gates Field Effect Transistors (IGFETs).

In materials science, it is a common knowledge that the magnitude/size of $E_g$, will affect the optoelectronic as well as the photonic properties of the material. With addition of element(s) into a lattice (through doping or full/partial substitution), a change in $E_g$ can be achieved. The adjustment of $E_g$ in insulating/semiconducting compounds and the impact of such adjustment on the electronic, optoelectronic and the photonic properties of the material must be understood in order to design new functional devices. In the present theoretical work, the bandgap of the rock salt MgO (an insulator) is varied systematically by alloying with that of CdO (a semi-metal). In order to understand the optoelectronic nature of these alloys, their structural, electronic and optical properties are investigated.

## 2. CALCULATION METHODS

All calculation is performed using the plane-wave pseudo-potential Density Functional Theory (DFT), of which its one particle Schrödinger equation is written as [14, 15]:

$$\left[-\frac{1}{2}\nabla^2 + V_c(r) + \mu_{xc}(r)\right]\psi_i(r) = \varepsilon\psi_i(r), \quad (1)$$

where $-\frac{1}{2}\nabla^2$ is the kinetic energy, $V_c(r)$ is the Coulomb energy and $\mu_{xc}(r)$ is the exchange-correlation. The solutions to (1) are one-particle wave-functions related to the total electron density as:

$$\rho(r) = \sum_i n_i \,|\psi_i(r)|^2, \quad (2)$$

where $n_i$ is the $i^{th}$ state occupation number. The unknown wave-function $\psi_i(r)$, is usually expanded in terms of known basis functions $\varphi_j(r)$with unknown linear expansion coefficients $c_{ij}$ as:

$$\psi_i(r) = \sum_i c_{ij}\,\varphi_j(r), \quad (3)$$

The unknown coefficients $c_{ij}$ are obtained by applying variational procedure to solve a matrix of the form:

$$(H - \varepsilon S)c = 0, \quad (4)$$

where *H* and *S,* have matrix elements:

$$H_{ij} = \int \varphi_i^* \left[-\frac{1}{2}\nabla^2 + V_c(r) + \mu_{xc}(r)\right]\varphi_j(r)dr \quad (5)$$

$$S_{ij} = \int \varphi_i^*(r)\varphi_j(r)dr \quad (6)$$

in which $\varepsilon$ is the eigenvalue and *c* is the coefficients that are solution to the column vector. To obtain the eigenvalues and the coefficients, the matrix in (4) has to be diagonalized. All the equations in (1) – (6) are solved using the Quantum Espresso (QE) computer code [16]. The Vanderbilt-type ultra-soft pseudo-potential (USPP) [17] is used for electron-ion interactions. The exchange and correlation effect in the DFT are treated with the generalized gradient approximation (GGA) of Perdew–Burke–Ernzerhof [18]. A convergence threshold of $10^{-3}$ Ry/a.u. is placed on the ground-state energy during structure optimization. The adopted integration scheme over irreducible Brillouin zone is that of Monkhorst and Pack [19]. The lattice parameter and bulk modulus of $\mathrm{Cd}_{1-x}\mathrm{Mg}_x\mathrm{O}$ $(0 \le x \le 1)$ are evaluated from a fit of the energy-volume data to an equation of state [20] given as:

$$E(V) = E_0 + \frac{B_0 V}{B_0'}\left(\frac{\left(V_0/V\right)^{B_0'}}{B_0'-1} + 1\right) - \frac{B_0 V_0}{B_0'-1}, \quad (7)$$

where $E_0$ is the total energy of the supercell, $V$ is the unit volume, $B_0$ is the bulk modulus at zero pressure and $B_0'$ is the derivative of bulk modulus with pressure.

There is a relationship between the optical properties of a material and its dielectric function ($\epsilon$). The two parts to the dielectric function; the real and the imaginary parts are given as:

$$\epsilon(\omega) = \epsilon_1(\omega) + i\epsilon_2(\omega) \quad (8)$$

For the $Cd_{1-x}Mg_xO$ $(0 \leq x \leq 1)$ mixed compounds, the imaginary and the real parts can be calculated using [21, 22]:

$$\epsilon_2(\omega) = \frac{8}{2\pi\omega^2}\sum_{nn'}\int |pnn'(k)|^2 \frac{dSk}{\nabla\omega nn'(k)} \quad (9)$$

$$\epsilon_1(\omega) = 1 + \frac{2}{\pi}p\int_0^\infty \frac{\omega'\epsilon_2(\omega')}{\omega'^2 - \omega'^2}d\omega' \quad (10)$$

The refractive index can be calculated in terms of the real and the imaginary parts of the dielectric function by the following relation:

$$n(\omega) = \frac{1}{\sqrt{2}}\left[\{\epsilon_1(\omega)^2 + \epsilon_2(\omega)^2\}^{1/2} + \epsilon_1(\omega)\right]^{1/2} \quad (11)$$

and the absorption coefficient can be calculated by:

$$\propto(\omega) = \frac{\omega\epsilon_2(\omega)}{c} \quad (12)$$

Since all the functions in (8) – (11) depend on the electronic band structure, they can thus be easily evaluated from DFT calculations.

## 3. RESULTS AND DISCUSSION

The composition of Cd at a step of 0.25 in MgO resulted significantly into different crystal structure as shown in Fig. 1 (b) – (d). The atomic mass of Cd (112.41 g) is quite large, compared to that of Mg (24.31 g). This is suspected to have impacted on the atomic volumes and therefore the change in the crystal structure of $Cd_{1-x}Mg_xO$ $(0 \leq x \leq 1)$, as the concentration of Mg increases from 0 to 100%. Due to the volume change, the space group of the structure obtained also changed from Fm-3m to Pm-3m at ratio 3:1 (see Fig. 1b) of Cd to Mg ($Cd_{0.75}Mg_{0.25}O$), A similar space group is obtained at ratio 1:3 (see Fig. 1d) of Cd to Mg ($Cd_{0.25}Mg_{0.75}O$). At a ratio of 1:1 of Cd to Mg ($Cd_{0.50}Mg_{0.50}O$), the structure changes from cubic to tetragonal as shown in Fig. 1(c).

The calculated lattice constant (LP), bulk modulus ($B_0$) and the band-gaps ($E_g$) are presented in Table 1. The experimental data on the binary compounds (MgO and CdO) deviates from theoretical results. This is not surprising because theoretical bandgap data are usually underestimated by DFT calculation methods. The trend seen in LP as Cd substitutes Mg is expected, as the atomic radius of Cd (144 pm) is slightly higher than for Mg (141 pm). However, despite the systematic variation in the LP, a huge difference can be seen in the bulk modulus as Cd supplants Mg in MgO. When 25% Mg is substituted with Cd in MgO ($Cd_{0.25}Mg_{0.75}O$), $B_0$ rose from 149.3 GPa to 614.2 GPa (an increment that is well above 300%). On the Vickers scale, $B_0$ relates directly with materials hardness [23]. Thus, it

can be concluded that Cd in MgO is an excellent hardener, where the level of hardness depends majorly on Cd content.

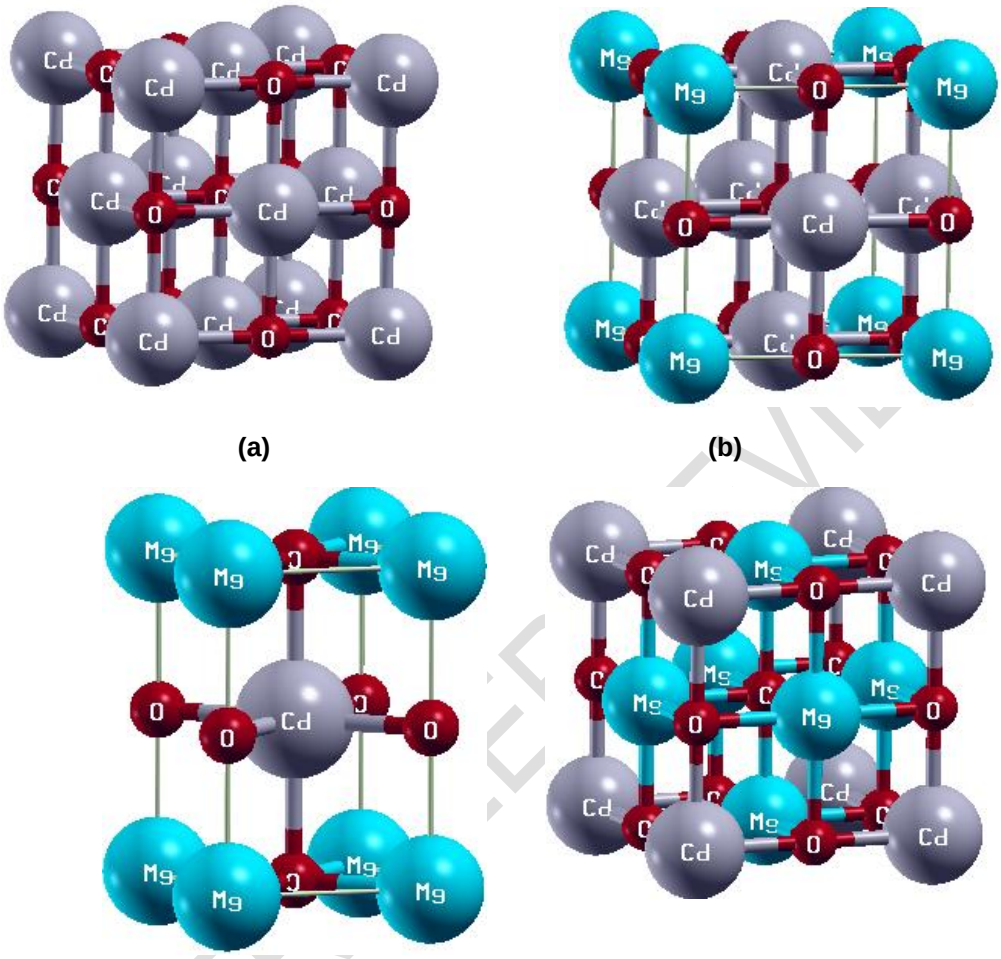


**Fig. 1. Crystal structure of (a) CdO, (b) $Cd_{0.75}Mg_{0.25}O$ (c) $Cd_{0.5}Mg_{0.5}O$ and (d) $Cd_{0.25}Mg_{0.75}O$**

The band structure for MgO and CdO are shown in figure 2. The projected density of states is also presented alongside in order to understand bonding and the origin of these bands. It is evident from Fig. 3(a) that MgO is an insulator. Its bands are scanty both in the conduction and the valence band. Also, a wide bandgap is seen in its band diagram. On the other hand, a narrow bandgap coupled with denser bands are seen in the band diagram of CdO (see figure 3(b)). Both MgO and CdO are direct bandgap materials. The conduction and valence bands of CdO are influenced by Cd-2s, Cd-3p and O-2p orbitals. In MgO, the activities at the valence band are influenced solely by O-2p while it is influenced at the conduction band by

Mg-3s and O-2p orbitals. Going by the Pauling Scale, the electro-negativity difference between Cd (1.69), Mg (1.31) and O (3.04) indicates that covalent bond dominates in CdO than in MgO. When this information is combined with their respective high $B_0$ values, CdO and MgO are hard and brittle materials.

Table 1: Calculated lattice constants (LP), bulk modulus ($B_0$) and bandgap ($E_g$) for mixed compounds of $Cd_{1-x}Mg_xO$ ($0 \leq x \leq 1$). Experimental data are in bracket and are from [24].

| Alloy | LP (Å) | $B_0$ (GPa) | $E_g$ (eV) |
|---|---|---|---|
| MgO | 4.249 | 149.3 | 3.216 [7.00] |
| $Cd_{0.25}Mg_{0.75}O$ | 4.391 | 614.2 | 1.185 |
| $Cd_{0.5}Mg_{0.5}O$ | 4.431; 4.775 | 600.0 | 0.684 |
| $Cd_{0.75}Mg_{0.25}O$ | 4.476 | 689.3 | 0.013 |
| CdO | 5.372 | 29.30 | 0.303 [0.85] |

The band diagram for the compounds in which the ratio of Mg to Cd is 1:3 ($Cd_{0.75}Mg_{0.25}O$) and 3:1 ($Cd_{0.25}Mg_{0.75}O$) are shown in Fig. 3, while that for which Mg to Cd is in ratio 1:1 is shown in Figure 4. It can be predicted from Figures 3 and 4 that $Cd_{1-x}Mg_xO$ ($0.25 \leq x \leq 0.75$) mixed compounds are indirect bandgap materials. The nature of the bandgap is not affected even as Cd substitutes Mg. Rather, the bandgap decreases from 3.216 eV (for MgO) down to 0.134 eV (for $Cd_{0.75}Mg_{0.25}O$). In Figure 3(a), O-2p orbital is solely responsible for bonding and the band character at the valence and conduction bands. It is therefore interesting to see that while Cd-2s, Cd-3p and O-2p are responsible for orbital hybridization in CdO, the story is quite different when one Cd is replaced with Mg (giving $Cd_{0.75}Mg_{0.25}O$). The interchange of state seen is due to a change in the nature of the bonding. The electronegativity of Cd > Mg, hence, a decrease in the dominant nature of covalent bonding is expected with increase in Mg content. In this light, O-2p dominates at the valence band, while Cd-3p and O-2p are responsible for the band character at the conduction band in $Cd_{0.25}Mg_{0.75}O$ (Fig. 3(b)). Likewise, at 50% composition of Mg to Cd in $Cd_{0.5}Mg_{0.5}O$, O-2p dominates at the valence band, while Cd-3p and O-2p are responsible for the band character at the conduction band. In comparison with MgO, partial covalent bonding is

predominant in $Cd_{1-x}Mg_xO$ $(0.25 \leq x \leq 0.75)$, hence the reason for their respective high $B_0$

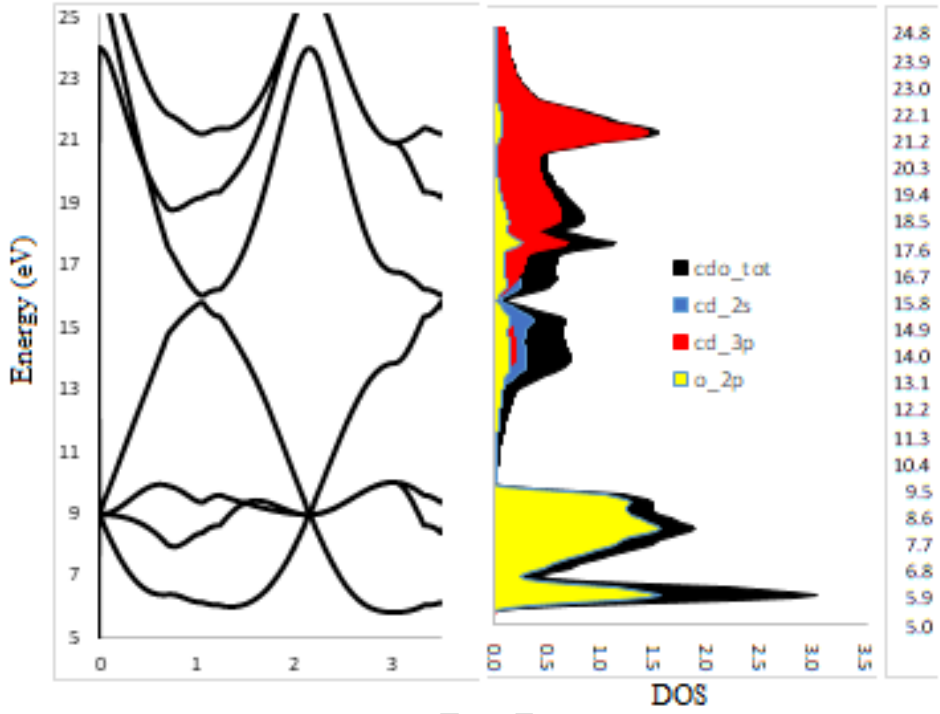


values.

(a)

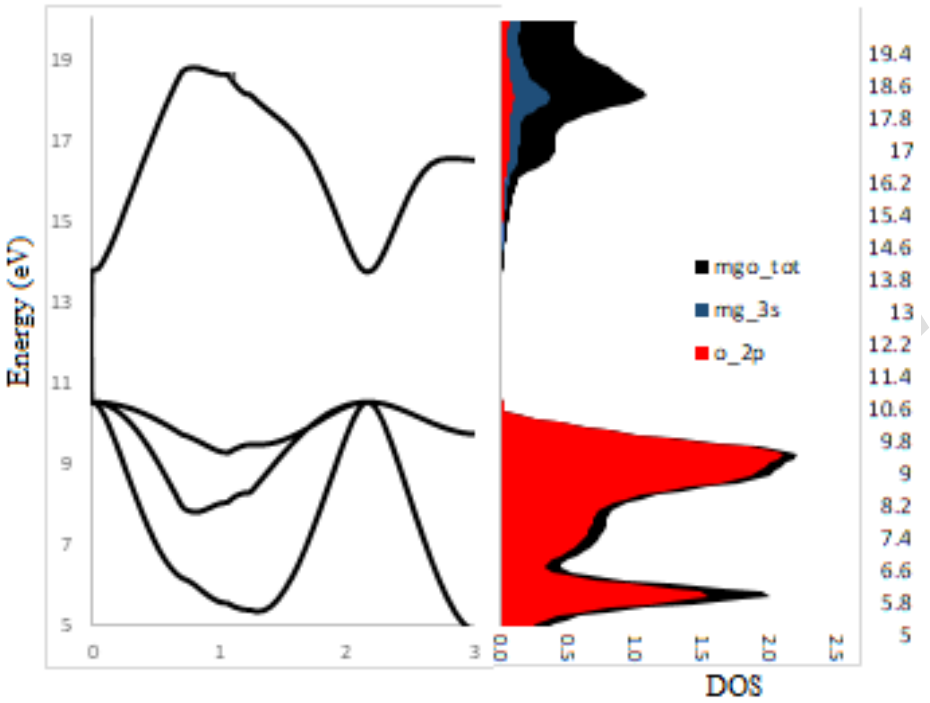


(b)

**Fig. 2. Calculated band structure for (a) CdO and (b) MgO**

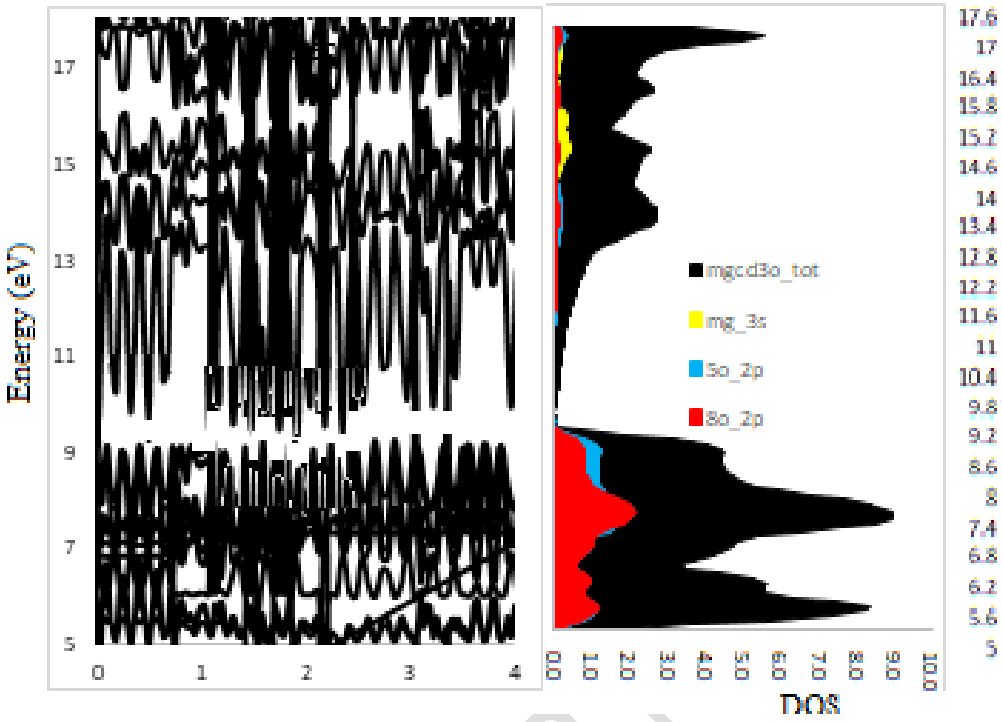


(a)

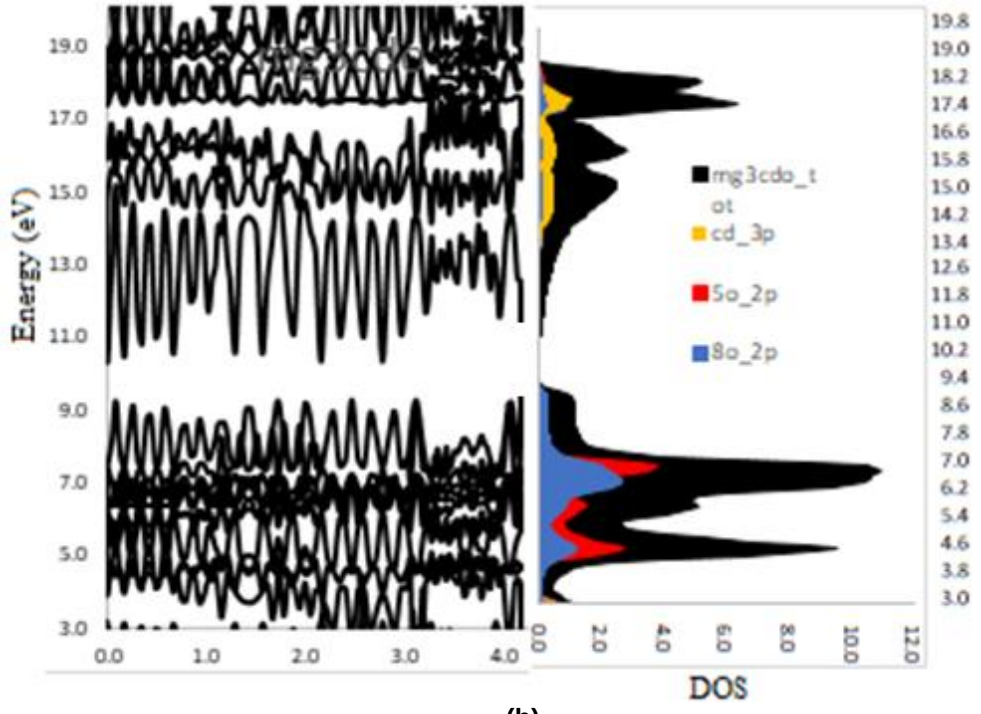


(b)

**Fig. 3. Band structure calculation for (a) $MgCd_3O$, (b) $Mg_3CdO$ and (c) MgCdO.**

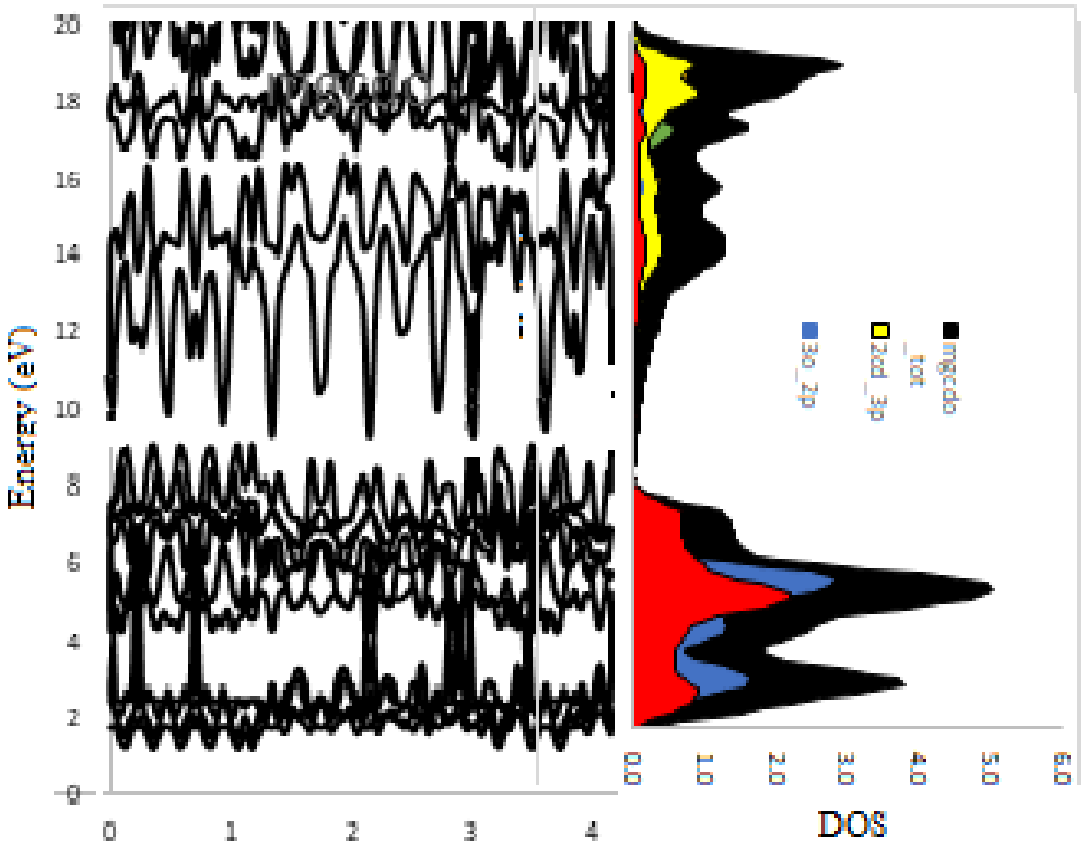


**Fig. 4. Band structure calculation for MgCdO.**

Materials with bandgap ($E_g$) are required for optoelectronic applications. Available evidence [25, 26] has shown that materials with $E_g \leq 3.1$ eV work well for devices working within the visible region of energy spectrum while those with $E_g > 3.1$ eV are good for devices working within the UV region. The mixture of MgO (an insulator) with CdO (a semiconductor) in $Cd_{1-x}Mg_xO$ $(0 \leq x \leq 1)$ stoichiometry should provide promising devices whose bandgap would vary between 0.85 and 7.00 eV. The calculated $E_g$ results in Table 1, especially for the binary compounds (MgO and CdO) are lower compared to experimental $E_g$. This is to be expected because DFT usually underestimate $E_g$. Despite the underestimation, it is predicted that $Cd_{1-x}Mg_xO$ $(0.25 \leq x \leq 0.75)$ compounds should suite optoelectronic applications both in the visible and ultraviolet (UV) regions. To understand the prominent variations in the optical absorption behavior of the materials, the calculated dielectric function (the imaginary part) in the 0–25 eV energy range is shown in Fig. 5. It is evident from this figure that the absorption of MgO is somewhat between 4.8 and 18 eV with its critical point at about 11.2 eV. As the concentration of Cd increases, the width and critical points of the absorption region shift toward lower energy, except for $Cd_{0.5}Mg_{0.5}O$ where the critical point is maintained at almost 11.2 eV and this may be attributed to the structural change (cubic to tetragonal) that occurred at that composition.

A plot of $n(\omega)$ for $Cd_{1-x}Mg_xO$ $(0 \leq x \leq 1)$ is shown in Fig. 6. There are two things that are obvious here. First, a broad spectrum of $n(\omega)$ over wide energy range is noted. The

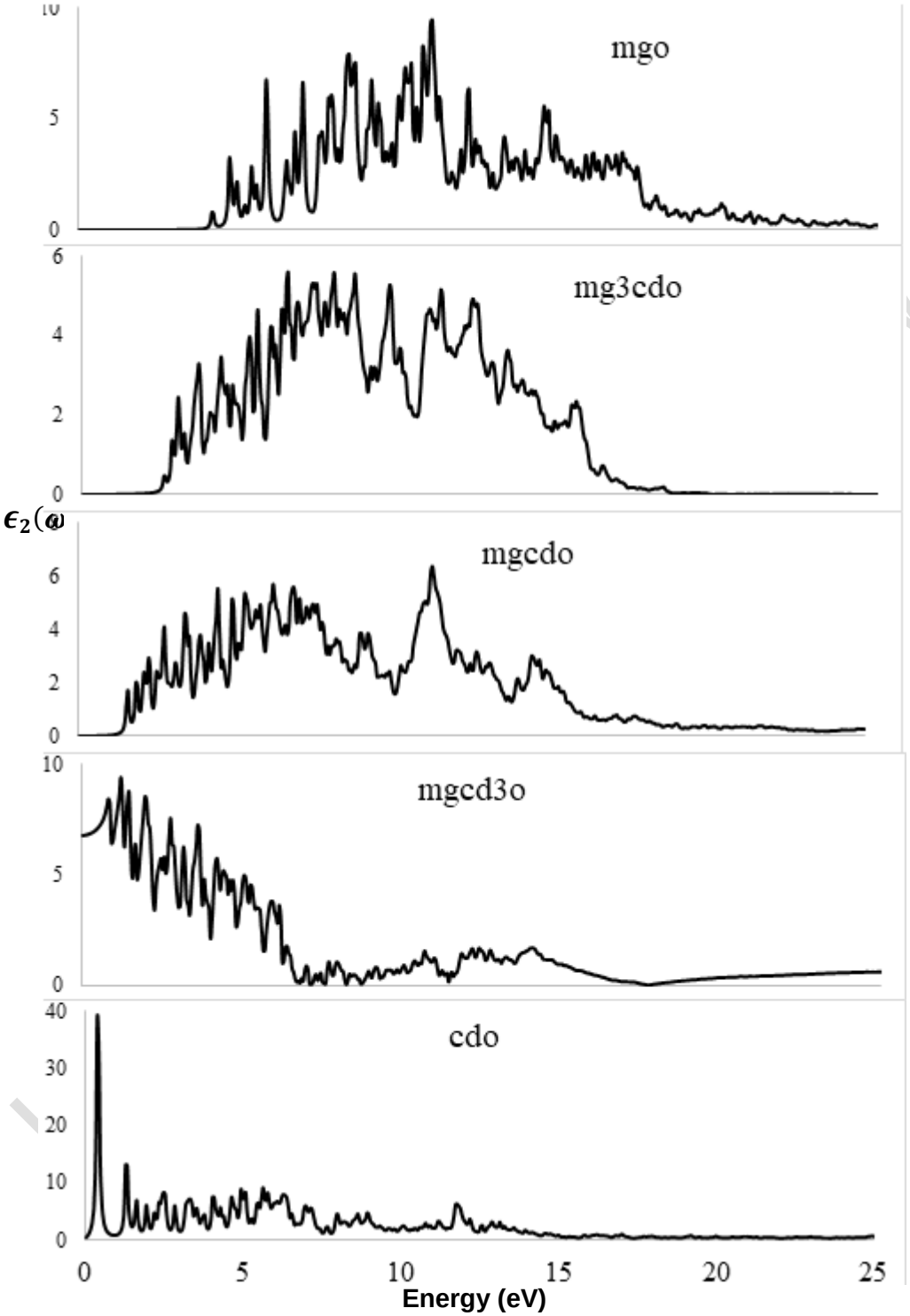


**Fig. 5. Frequency dependent imaginary part of dielectric functions of $Cd_{1-x}Mg_xO$ ($0 \leq x \leq 1$)**

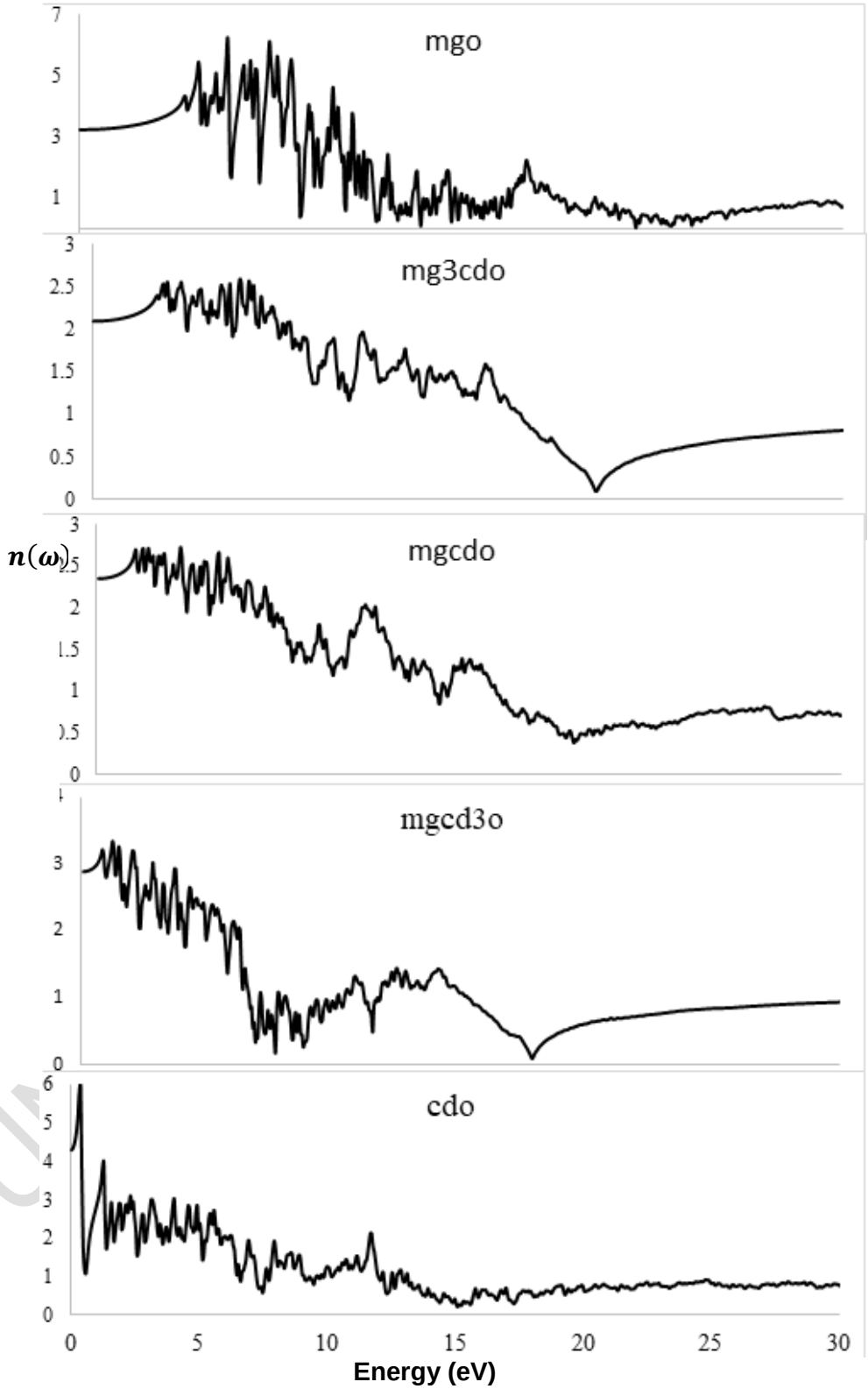


**Fig. 6. Frequency dependent refractive indices of $Cd_{1-x}Mg_xO$ ($0 \leq x \leq 1$)**

$n(\omega)$ maxima shift to lower energy region with increase in Cd concentration. Secondly, $n(\omega)$ drops below unity at certain energy ranges. Any $n(\omega)$ lesser than unity means that $v_g$ (the group velocity) of the wave packet is larger than $c$ ($v_g = \frac{c}{n}$). In other words, at $n(\omega) < 1$, $v_g$ would shifts to the negative domain and hence, the material becomes superluminal for high energy incident photons [27, 28].

## 4. CONCLUSION

For the first time, the Density functional calculation method have been performed to investigate the structure and the optoelectronic properties of compounds formed from systematic mixture of MgO and CdO in ratio $\mathrm{Cd}_{1-x}\mathrm{Mg}_x\mathrm{O}$ $(0 \leq x \leq 1)$. At equal concentration of Cd to Mg, structure change from cubic to tetragonal is predicted. The bonding nature in the materials significantly varies with Cd resulting in extremely hard materials. All the mixed compounds have indirect bandgaps according to their calculated band structure. It can be concluded that with appropriate experimental procedure, the material can be used in optoelectronic applications working in the visible and UV regions of spectrum.

## Competing interests

The authors hereby declare that no competing interest exists.



## REFERENCES

[1] Li M, Wang X, Li H, Di H, Wu X, Fang C, et al. Preparation of photoluminescent single crystalline MgO nanobelts by DC arc plasma jet CVD. Applied Surface Science, (2013) 274. 188-194.

[2] Li YB, Bando Y, Sato T. Preparation of network-like MgO nanobelts on Si substrate . Chemical Physics Letters. 2002; 359:141-145.

[3] Kim J, Gila BP, Mehandru R, Johnson JW, Shin JH, Lee KP et al. Electrical characterization of GaN metal oxide semiconductor diodes using MgO as the gate oxide, GaN and Related Alloys. Proc. Research Society Symposium. 2002; 693:699-713.

[4] Hayashi K, Matsuishi S, Kamiya T, Hirano M, Hosono H. Light-induced conversion of an Insulating refractory oxide into a persistent electronic conductor. Nature. 2002**;** 419(6906):462-5.

[5] Liu H, Tse JS, Mao H. Stability of rock salt phase of zinc oxide under strong compression : synchrotron xray diffraction experiments and first-principles calculation studies. Journal of Applied Physics. 2006;100(9):5.

[6] Ismail RA. Improved characteristics of sprayed CdO films by rapid thermal annealing. J. Mater. Sci.: Mater. Electron. 2009;20:1219.

[7] Dakhel AA, Ali-Mohamed AY. Optical and transport phenomena in CdO:La films prepared by sol-gel method. J. Sol–Gel Sci. Technol. 44 (2007) 241 - 247.

[8] Dyachenko AV, Opanasuyk AS, Kurbatov DI, Kuznetnov, Cheong H. Effect of substrate temperature on substructural and properties of MgO thin films. Functional Materials, 22 (2015): 1 – 7.

[9] Wang WB, Yang Y, Yanguas-Gil A, Chang NN, Girolami GS, and Abelson JR. Highly conformal magnesium oxide thin films by low-temperature chemical vapor deposition from $Mg(H_3BNMe_2BH_3)_2$ and water. Appl. Phys. Lett. 2013;102:101605.

[10] Parkin SSP, Kaiser C, Panchula A. Rice PM, Hughes B, Samant M et al. Giant tunnelling magnetoresistance at room temperature with MgO (100) tunnel barriers. Nat. Mater. 2004;3:862.
[11] Ikeda S, Miura K, Yamamoto H, Mizunuma K, Gan HD, Endo M et al. A perpendicular-anisotropy CoFeB–MgO magnetic tunnel junction. Nat. Mater. 2010;9:721.
[12] Fujii E, Tomozawa A, Takayama R, Nomura K, Murata A, Hirasawa T et al. Preparation of (001)-oriented Pb(Zr,Ti)O/sub 3/ thin films and their piezoelectric applications. IEEE Transactions on Ultrasonics, Ferroelectrics, and Frequency Control. 2007;4(12):2431.
[13] Peidong Y. and Lieber CM. Nanorod-Superconductor Composites: A Pathway to Materials with High Critical Current Densities. Science. 1996;273:1836.
[14] Kohn W and Sham LJ. Self-Consistent Equations Including Exchange and correlation effects. Physical Reviews A. 1965;140:1133-1139.
[15] Hohenberg P and Kohn W. Inhomogeneous Electron Gas. Physical Reviews B. 1964;136:864-875.
[16] Giannozzi P, Baroni S, Bonini N, Calandra M, Car R, Cavazzoni C et al. Quantum Espresso: a modular and open-source software project for quantum simulations of materials Journal of Physics.Condensed Matter. 2009;21**:**395502.
[17] Vanderbilt D. Soft self-consistent pseudopotentials in generalized eigenvalue formalism. Phys. Rev. B. 1990;41**:**7892-7895.
[18] Perdew, JP, Burke K, and Ernzerhof M. Generalized Gradient Approximation Made Simple.Physical Review Letters. 1996;77:3865.
[19] Monkhorst HJ and Pack JD. Special points for Brillouin-zone integrations. Physical Reviews B. 1976;**13:**5188 – 5192.
[20] Murnaghan FD. The Compressibility of Media under Extreme Pressures Proc. Natl. Acad. Sci. USA.1994; 30(9):244-247.
[21] Wooten F. Optical Properties of Solids, Academic Press, New York, 1972.
[22] Fox M. Optical Properties of Solids, Oxford University Press, 2001.
[23] Tian Y, Xu B, Zhao Z. Microscopic theory of hardness and design of novel superhard crystals Int. J. Refract. Met. Hard Mater. 2012**;**33:93–106.
[24] Khan I, Iftikhar Ahmad, Amin B, Murtaza G, Ali Z. Bandgap engineering of $Cd_{1-x}Sr_xO$. Physica B.2011;406:2509 – 2515.
[25] Gfroerer TH, Priestley LP, Weindruch FE, Wanless MW. Defect-related density of states in low-bandgap $In_xGa_{1-x}As/InAs_yP_{1-y}$ double heterostructures grown on InP substrates. Appl. Phys. Lett. 2002; 80: 4570.
[26] Benkhedir ML, Aida MS, Stesmans A, Adriaenssens GJ. Experimental study of the density of states in the band gap of a-Se. J. Optoelectron. Adv. Mater. 2005;7 329 - 332.
[27] Penn DR. Wave-Number-Dependent Dielectric Function of Semiconductors. Phys. Rev. 1962;128: 2093.
[28] Wang LJ, Kuzmich A, Dogariu A. Gain-Assisted Superluminal Light Propagation Nature, 2000;406:277-283.